Theoretical Analyses of the Effects on the Linear and Quadratic Nonlinear Optical Properties of *N*-Arylation of Pyridinium Groups in Stilbazolium Dyes

Benjamin J. Coe,*,† David Beljonne,‡ Henryk Vogel,‡ Javier Garín,§ and Jesús Orduna§

School of Chemistry, University of Manchester, Oxford Road, Manchester M13 9PL, U.K., Laboratory for Chemistry of Novel Materials, Centre for Research on Molecular Electronics and Photonics, University of Mons-Hainaut, place du Parc 20, B-7000 Mons, Belgium, and Departamento de Química Orgánica, ICMA, Universidad de Zaragoza-CSIC, E-50009 Zaragoza, Spain

Received: July 7, 2005; In Final Form: September 6, 2005

N-Arylation of the pyridinium electron acceptor unit in stilbazolium chromophores has been found by previous experimental hyper-Rayleigh scattering and electronic Stark effect (electroabsorption) spectroscopic studies to lead to substantial increases in the static first hyperpolarizability β_0 (Coe, B. J. et al. *Adv. Funct. Mater.* **2002**, *12*, 110; **2003**, *13*, 347). We show here that INDO/SCI calculations on the isolated cations *trans*-4′-(dimethylamino)-*N*-R-4-stilbazolium (R = methyl **1**, phenyl **2**, 2,4-dinitrophenyl **3**, or 2-pyrimidyl **4**) predict only slight red-shifts in the energy of the intramolecular charge-transfer (ICT) transition and accompanying relatively small changes in β_0 on moving along the series. The inclusion of acetonitrile solvent using a polarizable continuum model affords a somewhat better agreement with the experimental data, especially the red-shifting of the ICT transition and the increase in β_0 on going from **1** to **4**. Time-dependent density functional theory (TD-DFT), finite field, and coupled perturbed Hartree−Fock calculations reproduce even more closely the empirical data and trends; the latter two approaches lead to the highest quadratic nonlinear optical (NLO) response of the studied chromophores for **3**, for which the predicted β_0 is ca. 50−100% larger than that of the analogous *N*-methylated cation **1**. Although the TD-DFT and INDO/SCI approaches give quite different results for ground- and excited-state dipole moments, the overall conclusions of these two methods regarding the ICT absorption and NLO responses are similar.

Introduction

Over recent years, organic nonlinear optical (NLO) materials have been intensively investigated, primarily for potential applications in advanced optoelectronic and all-optical data processing technologies.[1] The range of compounds studied is now very broad and includes salts such as stilbazolium species.[2] Attractive features of the latter type of materials include the use of counterion variations to modify crystal packing, potentially affording noncentrosymmetric macroscopic structures which are essential for bulk quadratic (second-order) NLO effects. Crystalline salts also offer inherently greater stabilities and higher chromophore number densities when compared with alternative NLO materials such as poled polymers. Quadratic NLO effects, which hold the most immediate promise for practical applications, derive at the molecular level from first hyperpolarizabilities β. The tuning and maximization of β responses has hence been a major focus of much recent research work, and such studies with charged chromophores have been greatly aided by the development of the hyper-Rayleigh scattering (HRS) technique.[3]

By using a combination of HRS and electronic Stark effect (electroabsorption)[4] spectroscopic measurements on dipolar ruthenium(II) complexes of pyridyl ligands, we have found that species with *N*-arylpyridinium electron acceptor groups possess static first hyperpolarizabilities β_0 which are 2−3 times larger than those of their *N*-methyl analogues.[5] Related studies with stilbazolium-type compounds have confirmed that such a β_0-enhancing effect is also observed in purely organic chromophores,[6] and crystalline materials displaying very pronounced second harmonic generation activity have been identified.[6a,c] It is clearly of interest to develop a fuller physical understanding of the origins of the effects of pyridinium *N*-arylation in such compounds, by recourse to MO theory. Previous INDO/SCI calculations on some Ru^{II} pentaammine complexes failed to reproduce the observed increases in β_0,[5d] predicting instead that the *N*-arylated chromophores have *smaller* NLO responses when compared with their methylated counterpart. However, subsequent time-dependent density functional theory (TD-DFT) studies on some related complexes by Lin et al. have afforded results which are more consistent with the empirical observations.[7] Our present theoretical investigations focus on the well-studied *N*-methyl stilbazolium chromophore **1** and its three *N*-arylated analogues **2**−**4**.[6a]

Experimental Section

INDO/SCI Calculations. The geometries of cations **1**−**4** were determined by the semiempirical method AM1[8] using the program package MOPAC. All molecules were fully optimized, and frequency analysis showed all structures to be minima on the potential energy surfaces. The intramolecular charge-transfer (ICT) transition energies, transition dipole moments, and state dipole differences were derived from the INDO calculations taking into account configuration interaction (CI). For the CI calculations, all the singly substituted excitations over all

* Corresponding author. Tel: +44 161 275 4601. Fax: +44 161 275 4598. E-mail: b.coe@man.ac.uk.
† University of Manchester.
‡ University of Mons-Hainaut.
§ Universidad de Zaragoza.

10.1021/jp053721z CCC: $30.25
Published on Web 10/14/2005

TABLE 1: Experimental[a] and INDO/SCI-Derived Visible Absorption Maxima and First Hyperpolarizabilities for Cations 1−4

	λ_{max}, E_{max}[ICT] (nm, eV)			β_{1300} (10^{-30} esu)			β_0 (10^{-30} esu)			
cation	expt[b]	INDO/SCI	INDO/SCI[c]	HRS[b,d]	INDO/SCI	INDO/SCI[c]	HRS[b,d]	Stark[e]	INDO/SCI	INDO/SCI[c]
1	470, 2.64	485, 2.56		60	733		25	118	260	
2	504, 2.46	487, 2.55	492, 2.52	355	763	805	120	144	261	267
3	537, 2.31	486, 2.55	497, 2.49	370	901	846	100	181	324	283
4	553, 2.24	492, 2.52	498, 2.49	1015	846	912	230	159	283	295

[a] All measurements were made with PF_6^- salts. [b] In acetonitrile solutions at room temperature. [c] INDO/SCI calculated, with X-ray crystallographic dihedral angles (56°, 84°, and 12°, respectively for [**2**]PF_6, [**3**]PF_6, and [**4**]BPh_4).[6a,c] [d] Data taken from ref 6a. [e] In butyronitrile glasses at 77 K; data taken from ref 6c and derived by using the two-state equation $\beta_0 = 3\Delta\mu_{ge}(\mu_{ge})^2/2(E_{max})^2$ (perturbation series convention).[18]

TABLE 2: Results of INDO/SCI Calculations for Cations 1−4 Using DFT-Optimized Geometries

	λ_{max}[ICT] (nm)		E_{max}[ICT] (eV)		μ_{ge} (D)		$\Delta\mu_{ge}$ (D)		β_0 (10^{-30} esu)	
cation	vacuum	MeCN	vacuum	MeCN	vacuum	MeCN	vacuum	MeCN	vacuum	MeCN
1	507	474	2.44	2.62	12.4	11.6	11.5	11.4	255	179
2	506	470	2.45	2.64	13.0	12.3	11.5	10.7	255	163
3	518	*a*	2.39	*a*	13.6	*a*	11.0	*a*	297	*a*
4	517	512	2.40	2.42	13.5	13.5	11.0	11.2	283	280

[a] Not converged. Measured values at 77 K in butyronitrile (and used to derive Stark β_0 values in Table 1): μ_{ge} (D) = 9.1 (**1**); 9.4 (**2**); 9.5 (**3**); 9.5 (**4**). $\Delta\mu_{ge}$ (D) = 16.3 (**1**); 16.3 (**2**); 18.4 (**3**); 14.5 (**4**).[6c]

TABLE 3: Results of TD-DFT and CPHF Calculations for Cations 1−4

cation	λ_{max}, E_{max}[ICT] (nm, eV)	μ_{ge} (D)	f_{os}	$\Delta\mu_{ge}$ (D)	major contribution	β_0[FF-DFT][a] (10^{-30} esu)	β_0[CPHF][b] (10^{-30} esu)	β_0[TD-DFT][c] (10^{-30} esu)
1	468, 2.65	11.5	1.32	13.9	HOMO→LUMO	150	186	163
2	482, 2.57	12.6	1.55	14.0	HOMO→LUMO	189	226	197
3	840, 1.48	0.9	0.03	44.1	HOMO→LUMO	290	277	9
	472, 2.62	12.7	1.59	12.6	HOMO→LUMO+2			173
4	505, 2.45	13.1	1.60	16.7	HOMO→LUMO	259	263	279

[a] B3P86/LanL2DZ model Chemistry. [b] HF/LanL2DZ model Chemistry. [c] Calculated from the TD-DFT results by using the two-state equation $\beta_0 = 3\Delta\mu_{ge}(\mu_{ge})^2/2(E_{max})^2$.

π-orbitals were included (SCI). The zero frequency first hyperpolarizabilities β_{vec} (= β_0) were calculated by using the Sum-Over-States (SOS) approach on the basis of the SCI results. The term β_{vec} is usually employed in electric-field-induced second harmonic generation experiments and is the projection of β_{tot} along the dipole moment vector.

Hartree−Fock and DFT Calculations. All calculations were performed by using the Gaussian 03 program.[9] The molecular geometries were fully optimized with no restrictions by using the hybrid functional B3P86[10] and the LanL2DZ[11] basis set. The same model chemistry was used for TD-DFT and finite field (FF) calculations. Excited-state dipole moments were calculated by using the one particle RhoCI density. Molecular hyperpolarizabilities were also calculated by using the coupled perturbed Hartree−Fock (CPHF) method and the LanL2DZ basis set. The default Gaussian 03 parameters were used in every case. The β_0 values included in Table 3 are the zero frequency β_{tot} values from DFT calculations. Note that for dipolar molecules, β is aligned to the dipole moment and therefore $\beta_{vec} = \beta_{tot}$. Molecular orbital contours were plotted by using Molekel 4.3.[12]

Results and Discussion

Initially, we have carried out INDO/SCI calculations on the isolated cations **1**−**4**. The results of MO calculations have been reported previously for **1**,[13] **5**,[14] and for the neutral compound *trans*-4′-(dimethylamino)-*N*-(2-benzimidazolate)-4-stilbazolium (**6**),[15] but *N*-aryl stilbazolium cations have not yet been studied theoretically to our knowledge. The resulting first hyperpolarizabilities β_{vec} (= β_0) of **1**−**4** are shown in Table 1.

The INDO/SCI-calculated β_0 for **1** is similar to that previously reported (241 × 10^{-30} esu).[13b] However, the calculated β_0 values are rather larger than those derived from either the HRS or Stark measurements, and they also show only a very modest increase in moving from **1** to **4**. The latter result is unsurprising given that these calculations also predict that the ICT absorption maximum remains essentially constant throughout the series, whereas in practice a steady red-shifting is observed. One of the reasons for this marked disagreement between theory and experiment might be the conformation of the arylpyridinium group. Because the AM1 dihedral angles between the pyridyl and *N*-aryl rings differ from those observed in X-ray crystal structures,[6a,c] we have also carried out calculations with the optimized AM1 geometries but forcing the inter-ring dihedral angles to the X-ray values. The results of these calculations are also given in Table 1, but show only small differences from the data obtained when using the AM1 angles. Clearly, the initial INDO/SCI theoretical model does not accurately reproduce either the linear absorption or NLO properties of [**1**−**4**]PF_6 in solution. We have therefore carried out further calculations by using the optimized molecular geometries obtained via the DFT method (see below) and also incorporating acetonitrile solvent by using the polarizable continuum model (PCM).[16] The results of these calculations are shown, together with the corresponding data for the cations in a vacuum, in Table 2 ($\Delta\mu_{ge}$ is the dipole moment change associated with the ICT transition and μ_{ge} is the transition dipole moment). Unfortunately, it proved impossible to get the calculations for cation **3** to converge, probably because of the large dipoles induced by the $-NO_2$ groups.

It is interesting to note the close agreement between the INDO/SCI-derived (acetonitrile) and measured excitation energy for **1**. Although the INDO/SCI values of μ_{ge} and $\Delta\mu_{ge}$ do not agree very well with the experimental values, the β_0 values agree somewhat better with the corresponding Stark-derived data when

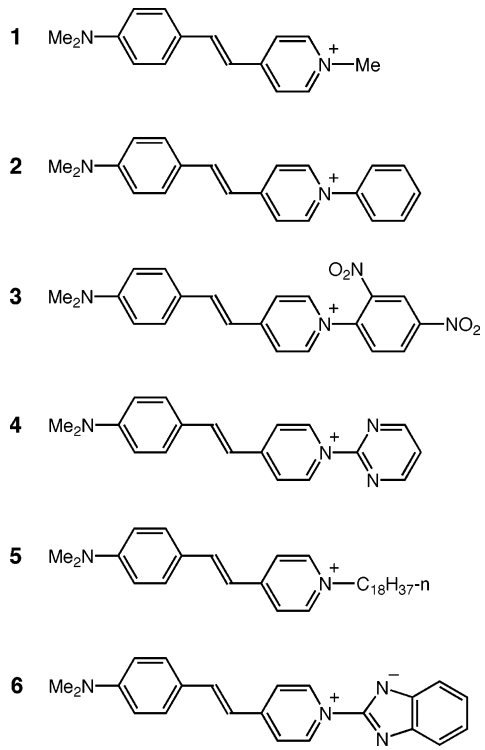

Figure 1. Chemical structures of the stilbazolium cations investigated, together with some related chromophores.[14,15]

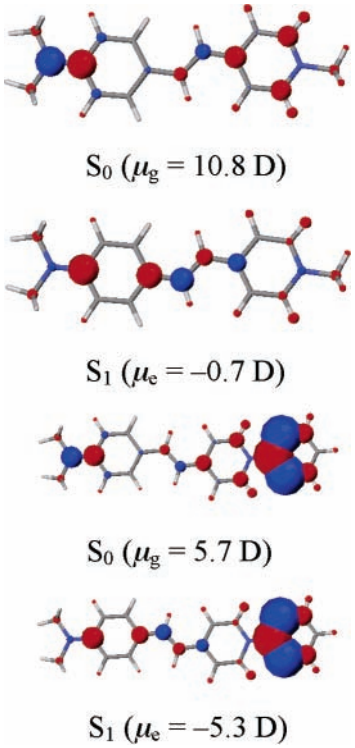

Figure 2. INDO/SCI-derived charge distributions of the electronic ground and first excited states for the cations **1** (top) and **4** (bottom) in a vacuum.

the solvent is taken into account. In particular, a considerably larger increase in β_0 is predicted on moving from **1** to **4** in acetonitrile when compared with the vacuum data. These results can be interpreted as follows. These molecules possess large ground-state dipole moments μ_g, especially **1** (although this is a somewhat undefined quantity for a charged system; the molecules were oriented along their principal axes of inertia in all cases). Moving from **1** to **4** results in a large decrease in μ_g, due to charge-transfer to the aryl unit on the acceptor side in **4** (Figure 2). The value of $\Delta\mu_{ge}$ is, in contrast, very similar for both cations. As expected from the larger dipole moment in the ground-state, the ICT transition in **1** is blue shifted when going from the gas phase to solution, hence rationalizing the smaller quadratic NLO response obtained in the latter case (according to a simple two-state model). In contrast, $|\mu_g| \sim |\mu_e|$ in **4**, yet the state dipoles have opposite signs, so that a much smaller shift in excitation energy is predicted for the latter molecule and the gas-phase and solution β_0 values are very close to one another. Overall, the increase in β_0 on moving from **1** to **4**, as predicted at the INDO/SCI level in acetonitrile, arises primarily from the lower transition energy to the ICT state together with the larger associated transition dipole moment. Such bathochromic and hyperchromic shifts when going from **1** to **4** are fully consistent with experiment.

Since we have previously found that TD-DFT and FF calculations reproduce relatively accurately the measured dipole and optical parameters for **1** and for its extended homologues with two or three *E*-CH═CH linkages,[17] it is clearly of interest to apply such computational methods to the *N*-aryl stilbazolium cations **2**−**4** and to compare the results with those obtained by using the more traditional INDO/SCI approach.

The optimization of the molecular geometries of cations **1**−**4** yielded fully planar (C_s) geometries for **1** and **4**, while the calculated dihedral angles between the pyridinium and *N*-aryl rings in **2** and **3** of 50° and 80°, respectively, are in a reasonably good agreement with those observed in the X-ray crystal structures.[6a,c] The calculation of optical properties was performed by using these optimized geometries. It is worth noting that ab initio calculations provide a very poor description of excited states and thus are useless when performing SOS computations, which are usually successful when using INDO/SCI. On the other hand, coupled methods such as CPHF or FF which compute the hyperpolarizability as the second derivative of the dipole moment are usually accurate when using ab initio methods, provided that an adequate basis set is employed. Unfortunately, these coupled methods give no information on the excited states involved and are not amenable to intuitive interpretations. The situation is even worse when using DFT methods, since the commonly used functionals present a bad asymptotic behavior and fail to calculate the hyperpolarizability of neutral or anionic molecules. Fortunately, cationic species (such as **1**−**4**) with a more compact electronic cloud are not affected by such bad asymptotic behavior, and their hyperpolarizabilities can be reasonably accurately calculated by DFT. The β_0 values calculated for **1**−**4** by using either a FF-DFT or CPHF model as well as the results of TD-DFT calculations are gathered in Table 3, and the MOs that contribute to the ICT transitions are depicted in Figure 3.

It can be seen that while the TD-DFT results are not quantitatively accurate, they provide a somewhat better description of the experimental observations than do the gas-phase INDO/SCI calculations, reproducing quite well the observed trends in the linear and NLO behavior. The calculated total bathochromic shift along the series **1**−**4** of 0.20 eV is not as high as that observed experimentally in acetonitrile solutions (0.4 eV) but is more realistic than the small values of ca. 0.05 eV obtained via the INDO/SCI method in a vacuum (Tables 1 and 2). However, when the solvent is included the corresponding INDO/SCI-derived shift is similar to that obtained from TD-DFT, although only the latter theoretical method also predicts a bathochromic shift on moving from **1** to **2**. In a similar manner, both the FF-DFT and CPHF calculations account for a noticeable

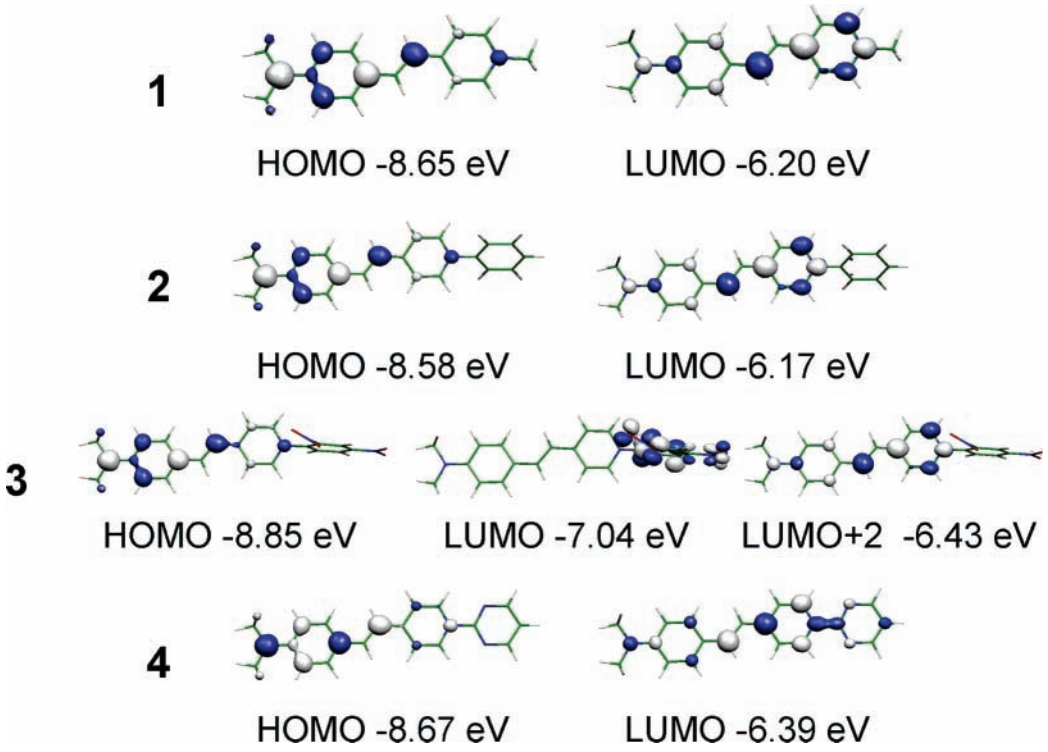

Figure 3. 0.05 Contour plots of the MOs involved in the ICT transitions for cations **1**−**4** calculated by B3P86/6-31G*.

and continual enhancement of β_0 along the series **1**−**4** that is only partly predicted by the INDO/SCI method (either in the gas phase or solution). However, all three theoretical approaches agree in predicting that the 2,4-dinitrophenyl (2,4-DNPh) chromophore **3** has the largest NLO response, although nonconvergence was found for this cation when incorporating the solvent into the INDO/SCI calculations. The latter conclusion also emerges from the Stark data, but not from the HRS results which indicate that **4** has the largest β_0. Hence, while the theoretical and experimental β_0 values do not agree closely, there are also clear differences between the corresponding values determined via either the Stark or HRS techniques. Furthermore, TD-DFT calculations such as these that do not include solvent effects can be expected to yield the correct experimental trends but not quantitative predictions of the transition energies or molecular hyperpolarizabilities (see below). It is interesting to note the close agreement between the INDO/SCI-derived (acetonitrile) and DFT-calculated μ_{ge} values for **1**, **2**, and **4** and also the corresponding and almost exact agreement for β_0 of **4**.

A more intuitive explanation of the effects caused by *N*-arylation in these stilbazolium dyes can be drawn from the results of our TD-DFT calculations and considering the parameters involved in the two-state model[18,19]

$$\beta_0 \propto \frac{\Delta\mu_{ge}(\mu_{ge})^2}{(E_{max})^2} \propto \frac{\Delta\mu_{ge} f_{os}}{(E_{max})^3}$$

where f_{os} is the oscillator strength. For the PF_6^- salts of cations **1**−**4**, the μ_{ge} and $\Delta\mu_{ge}$ values measured in butyronitrile at 77 K are given in the footnote for Table 2.[6c] It is apparent that TD-DFT somewhat overestimates the magnitude of μ_{ge}, but (with the exception of **4**) underestimates $\Delta\mu_{ge}$ for these chromophores. Although the excited-state dipole moments calculated by using the RhoCI density (and hence the $\Delta\mu_{ge}$ values) are probably inaccurate, the β_0 values derived by application of the two-state model to the TD-DFT results are (with the exception of **3**) in surprisingly good agreement with the outcomes of the FF-DFT and CPHF calculations (Table 3).

When comparing **1** and **2**, the topology of the DFT-derived MOs remains largely unchanged (Figure 3), but replacement of an *N*-Me with a *N*-Ph group gives rise to a reduced HOMO−LUMO gap and hence to a bathochromic shift in E_{max}. Furthermore, both f_{os} and $\Delta\mu_{ge}$ are (albeit only slightly for the latter quantity) larger in the more extended cation **2**, and all of these changes are responsible for an increased β_0 response.

The 2-pyrimidyl group in **4** has a much larger electronic influence than the phenyl group in **2** due to mixing of pyridine and pyrimidine π orbitals which yields a LUMO that spreads over these two heterocyclic rings and has a lower energy when compared to the LUMOs of **1** or **2**. This lowering of the LUMO gives rise to a decreased HOMO−LUMO gap and hence a lower E_{max} for **4**. The extension of the LUMO over the pyrimidine ring is responsible for extending the electron-transfer distance for the ICT transition and therefore leads to a larger $\Delta\mu_{ge}$. The calculations also predict a somewhat larger μ_{ge} for **4** when compared with **2**, and therefore all of the factors involved in the two-state approach account for an increased β_0 for **4** when compared with **1** or **2**. These observations parallel the INDO/SCI results, except that the latter do not predict an increase in $\Delta\mu_{ge}$ on moving from **1** to **4**. Notably, the results of the Stark measurements concur with the INDO/SCI treatment on this point.

The TD-DFT calculations give rise to a more complex picture for cation **3**, in which there is poor mixing of the π orbitals of the 2,4-DNPh group with the pyridine orbitals, probably due to the large twisting angle of 80° between the two rings. Compared to **1** or **2**, the acceptor 2,4-DNPh group stabilizes both the HOMO and the LUMO (that becomes LUMO+2) but makes little difference to the calculated energy gaps and the resulting transition energy (2.62 eV) lies between those calculated for **1** and **2**. A two-state picture based on this ICT transition cannot explain the increased β_0 of **3** when compared with **2**. In fact, the intense ICT transition in **3** displays a somewhat higher E_{max},

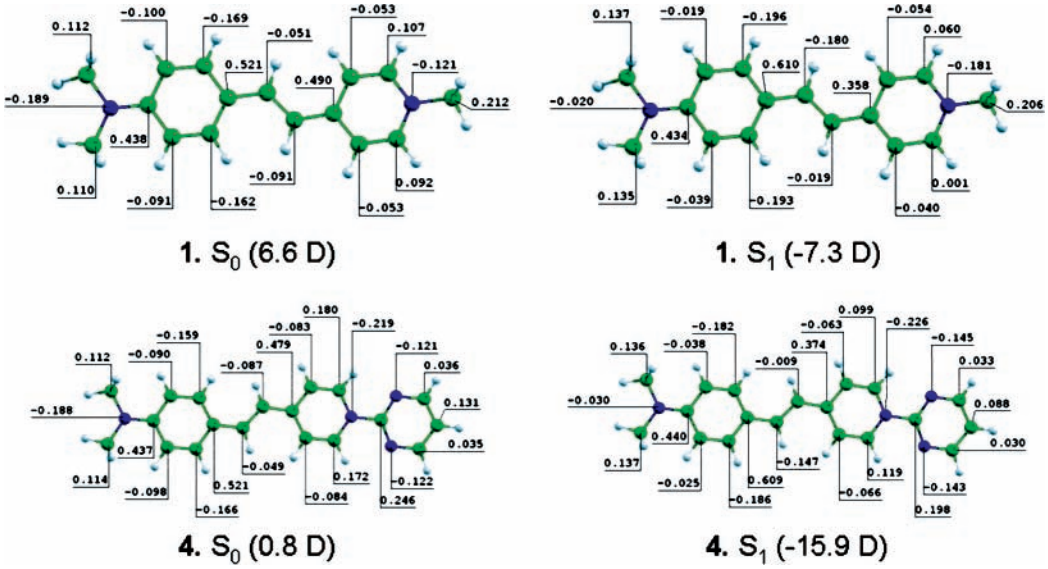

Figure 4. TD-DFT-derived charge distributions of the electronic ground and first excited states for the cations **1** (top) and **4** (bottom) in a vacuum. Because software limitations preclude plotting a graphical representation, the numerical values of the Mulliken charges are shown with hydrogens summed into heavy atoms.

TABLE 4: Results of TD-DFT Calculations for Cations 1−4 in Acetonitrile Using a PCM Model

cation	λ_{max}, E_{max}[ICT] (nm, eV)	μ_{ge} (D)	f_{os}	$\Delta\mu_{ge}$ (D)
1	476, 2.61	11.9	1.40	14.6
2	494, 2.51	13.1	1.63	14.7
3	1029, 1.21	2.75	0.03	44.4
	488, 2.54	13.1	1.66	12.6
4	529, 2.34	13.9	1.71	16.5

a similar μ_{ge} and a smaller $\Delta\mu_{ge}$. However, the calculations on **3** also predict an additional weak ICT band at very low energy due to a transition from the HOMO to the LUMO which is located on the 2,4-DNPh group. Considering that this is a very weak band and that TD-DFT often fails in the prediction of charge-transfer energies,[20] it is possible that this transition is hidden by the more intense HOMO→LUMO+2 band and is not observed experimentally, but the overlapping of these two bands causes an apparent shift to lower energy of the more intense band. Although this HOMO→LUMO transition has a very low μ_{ge}, it gives rise to a large $\Delta\mu_{ge}$ and is therefore expected to contribute to the larger β_0 of **3**.

In view of the beneficial effects of including solvation in the INDO/SCI model, we have also studied the effects of including the solvent in TD-DFT calculations, and the results of these studies are shown in Table 4. Recent TD-DFT studies with some zwitterionic chromophores related to **1** have predicted very marked effects on β responses of changing the solvent.[21] Unfortunately, with the present chromophores attempts to calculate FF or CPHF hyperpolarizabilities in solution give rise to unrealistically huge values. The data in Table 4 show some significant differences when compared with the corresponding vacuum data, but the overall trends are unchanged. Notably, the magnitude of the E_{max} decrease on moving from **1** to **4** has increased to 0.27 eV by including the solvent, reflecting more closely the experimental results. For several parameters, there is an excellent level of agreement between the calculated TD-DFT (acetonitrile) and INDO/SCI (acetonitrile) values. Interestingly, although these two techniques lead here to very similar overall results, the TD-DFT calculations in certain respects predict an opposed behavior to that described by INDO/SCI. For example, in contrast with INDO/SCI, TD-DFT predicts that the μ_g and μ_e values of **1** are very similar, although with different signs (μ_g = 6.6 D, μ_e = −7.3 D in a vacuum), and therefore the ICT absorption spectrum of **1** is little affected by the solvent. On the other hand, for **4** the predicted μ_e is larger than μ_g (−15.9 as opposed to 0.8 D in a vacuum), and therefore there is quite a large red-shift when the spectrum of the latter cation is calculated by TD-DFT in solution.

It is of interest at this point to consider the calculated charge distributions of the electronic ground and first excited states derived from TD-DFT (Figure 4), which may be compared with those obtained by using INDO/SCI (Figure 2). When considering the predicted ground-state charge distributions, it is interesting to note that while both methods yield about the same charge on the pyridinium unit (ca. 0.7 $|e|$ for both **1** and **4**), they give rise to a quite different charge distribution over the rest of the molecule, for example for **1** the charge on the phenyl ring is 0.44 $|e|$ at the TD-DFT level and only 0.16 $|e|$ at the INDO/SCI level.[22] Since the dipoles are calculated using the same convention by the two methods (namely with the center of inertia as origin of the axes frame), the fact that different results are provided by the two theoretical approaches is not an artifact but a consequence of the different charge distributions in the ground state. The results of preliminary solvatochromism measurements (performed for **1** and **4** in seven different solvents, Table 5) indicate that the lowest optical transition of **1**, and to a smaller extent that of **4**, is blue-shifted when going from a less polar solvent such as dichloromethane to a more polar

TABLE 5: ICT Maxima for the PF_6^- Salts of 1 and 4 in Common Organic Solvents

	λ_{max}, E_{max}[ICT] (nm, eV)							
salt	MeCN	DMF	DMSO	acetone	MeOH	$CHCl_3$	CH_2Cl_2	ΔE (eV)[a]
[**1**]PF_6	470, 2.64	470, 2.64	472, 2.63	474, 2.62	476, 2.61	504, 2.46	520, 2.38	0.25
[**4**]PF_6	553, 2.24	556, 2.23	556, 2.23	554, 2.24	558, 2.22	592, 2.09	600, 2.07	0.18

[a] Total energy shift on moving between MeCN and CH_2Cl_2.

solvent such as acetonitrile. This result is consistent with the trend observed at the INDO/SCI level when going from gas phase to acetonitrile solution (although the effect predicted for **4** is underestimated) but is in contrast with the TD-DFT results. Additional work on both the experimental and theoretical sides is needed to understand the origin of such a discrepancy.

Conclusions

Vacuum INDO/SCI calculations on the cations **1**−**4** predict only slight red-shifts in the energy of the ICT transition and accompanying relatively small changes in β_0 moving along the series **1**−**4**, in contrast with experiments which show a relatively large red-shift and increase in β_0. The extent of agreement with the experimental data is somewhat improved by the inclusion of an acetonitrile solvent continuum. TD-DFT, FF, and CPHF calculations reproduce even more closely the empirical data and trends, the latter two methods affording the highest quadratic NLO response for **3**, for which β_0 is predicted to be ca. 50−100% larger than that of **1**. The inclusion of solvent in the TD-DFT calculations also affords ICT energies which reflect more closely the experimental results. For several parameters, there is an excellent level of agreement between the values calculated via TD-DFT and INDO/SCI in acetonitrile. Although these two methods afford rather different predictions for ground- and excited-state dipole moments, they yield similar overall conclusions regarding the ICT absorptions and NLO responses.

Acknowledgment. We thank the EPSRC for support (Grant GR/M93864) and also MCyT-FEDER (BQU2002-00219) and Gobierno de Aragon-Fondo Social Europeo (E39). The work in Mons is partly supported by the Belgian Federal Services for Scientific, Technical, and Cultural Affairs (IUAP 5/3) and FNRS. D.B. is an FNRS Research Associate.

Supporting Information Available: Cartesian coordinates of DFT optimized geometries for the cations **1**−**4**. This material is available free of charge via the Internet at http://pubs.acs.org.

References and Notes

(1) (a) *Nonlinear Optical Properties of Organic Molecules and Crystals*; Chemla, D. S., Zyss, J.; Academic Press: Orlando, FL, 1987; Vols. 1 and 2. (b) *Molecular Nonlinear Optics: Materials, Physics and Devices*; Zyss, J.; Academic Press: Boston, 1994. (c) *Organic Nonlinear Optical Materials (Advances in Nonlinear Optics, Vol. 1.)*; Bosshard, Ch., Sutter, K., Prêtre, Ph., Hulliger, J., Flörsheimer, M., Kaatz, P., Günter, P.; Gordon & Breach: Amsterdam, The Netherlands, 1995. (d) *Nonlinear Optics of Organic Molecules and Polymers*; Nalwa, H. S., Miyata, S., Eds.; CRC Press: Boca Raton, FL, 1997. (e) *Nonlinear Optical Properties of Matter: From Molecules to Condensed Phases*; Papadopoulos, M. G., Leszczynski, J., Sadlej, A. J., Eds.; Kluwer: Dordrecht, 2005.

(2) Selected examples: (a) Marder, S. R.; Perry, J. W.; Schaefer, W. P. *Science* **1989**, *245*, 626. (b) Marder, S. R.; Perry, J. W.; Schaefer, W. P. *J. Mater. Chem.* **1992**, *2*, 985. (c) Marder, S. R.; Perry, J. W.; Yakymyshyn, C. P. *Chem. Mater*. **1994**, *6*, 1137. (d) Lee, O.-K.; Kim, K.-S. *Photonics Sci. News* **1999**, *4*, 9. (e) Kaino, T.; Cai, B.; Takayama, K. *Adv. Funct. Mater*. **2002**, *12*, 599. (f) Mohan Kumar, R.; Rajan Babu, D.; Ravi, G.; Jayavel, R. *J. Cryst. Growth* **2003**, *250*, 113. (g) Geis, W.; Sinta, R.; Mowers, W.; Deneault, S. J.; Marchant, M. F.; Krohn, K. E.; Spector, S. J.; Calawa, D. R.; Lyszczarz, T. M. *Appl. Phys. Lett.* **2004**, *84*, 3729. (h) Taniuchi, T.; Okada, S.; Nakanishi, H. *Appl. Phys. Lett.* **2004**, *95*, 5984. (i) Yang, Z.; Aravazhi, S.; Schneider, A.; Seiler, P.; Jazbinsek, M.; Günter, P. *Adv. Funct. Mater*. **2005**, *15*, 1072.

(3) (a) Clays, K.; Persoons, A. *Phys. Rev. Lett*. **1991**, *66*, 2980. (b) Hendrickx, E.; Clays, K.; Persoons, A. *Acc. Chem. Res.* **1998**, *31*, 675.

(4) (a) Liptay, W. In *Excited States*; Lim, E. C., Ed.; Academic Press: New York, 1974; Vol. 1, pp 129−229. (b) Bublitz, G. U.; Boxer, S. G. *Annu. Rev. Phys. Chem.* **1997**, *48*, 213.

(5) (a) Coe, B. J.; Essex-Lopresti, J. P.; Harris, J. A.; Houbrechts, S.; Persoons, A. *Chem. Commun.* **1997**, 1645. (b) Coe, B. J.; Harris, J. A.; Harrington, L. J.; Jeffery, J. C.; Rees, L. H.; Houbrechts, S.; Persoons, A. *Inorg. Chem*. **1998**, *37*, 3391. (c) Coe, B. J.; Harris, J. A.; Asselberghs, I.; Persoons, A.; Jeffery, J. C.; Rees, L. H.; Gelbrich, T.; Hursthouse, M. B. *J. Chem. Soc., Dalton Trans*. **1999**, 3617. (d) Coe, B. J.; Harris, J. A.; Brunschwig, B. S. *J. Phys. Chem. A* **2002**, *106*, 897. (e) Coe, B. J.; Jones, L. A.; Harris, J. A.; Sanderson, E. E.; Brunschwig, B. S.; Asselberghs, I.; Clays, K.; Persoons, A. *Dalton Trans*. **2003**, 2335. (f) Coe, B. J.; Harries, J. L.; Harris, J. A.; Brunschwig, B. S.; Coles, S. J.; Light, M. E.; Hursthouse, M. B. *Dalton Trans*. **2004**, 2935.

(6) (a) Coe, B. J.; Harris, J. A.; Asselberghs, I.; Clays, K.; Olbrechts, G.; Persoons, A.; Hupp, J. T.; Johnson, R. C.; Coles, S. J.; Hursthouse, M. B.; Nakatani, K. *Adv. Funct. Mater*. **2002**, *12*, 110. (b) Clays, K.; Coe, B. J. *Chem. Mater*. **2003**, *15*, 642. (c) Coe, B. J.; Harris, J. A.; Asselberghs, I.; Wostyn, K.; Clays, K.; Persoons, A.; Brunschwig, B. S.; Coles, S. J.; Gelbrich, T.; Light, M. E.; Hursthouse, M. B.; Nakatani, K. *Adv. Funct. Mater*. **2003**, *13*, 347.

(7) Lin, C.-S.; Wu, K.-C.; Snijders, J. G.; Sa, R.-J.; Chen, X.-H. *Acta Chim. Sinica* **2002**, *60*, 664.

(8) Dewar, M. J. S.; Zoebisch, E. G.; Healy, E. F.; Stewart, J. J. P. *J. Am. Chem. Soc*. **1985**, *107*, 3902.

(9) Gaussian 03, Revision B.05; Frisch, M. J.; Trucks, G. W.; Schlegel, H. B.; Scuseria, G. E.; Robb, M. A.; Cheeseman, V. G.; Montgomery, J. A.; Vreven, T., Jr.; Kudin, K. N.; Burant, J. C.; Millam, J. M.; Iyengar, S. S.; Tomasi, J.; Barone, V.; Mennucci, B.; Cossi, M.; Scalmani, G.; Rega, N.; Petersson, G. A.; Nakatsuji, H.; Hada, M.; Ehara, M.; Toyota, K.; Fukuda, R.; Hasegawa, J.; Ishida, M.; Nakajima, T.; Honda, Y.; Kitao, O.; Nakai, H.; Klene, M.; Li, X.; Knox, J. E.; Hratchian, H. P.; Cross, J. B.; Adamo, C.; Jaramillo, J.; Gomperts, R.; Stratmann, R. E.; Yazyev, O.; Austin, A. J.; Cammi, R.; Pomelli, C.; Ochterski, J. W.; Ayala, P. Y.; Morokuma, K.; Voth, G. A.; Salvador, P.; Dannenberg, J. J.; Zakrzewski, V. G.; Dapprich, S.; Daniels, A. D.; Strain, M. C.; Farkas, O.; Malick, D. K.; Rabuck, A. D.; Raghavachari, K.; Foresman, J. B.; Ortiz, J. V.; Cui, Q.; Baboul, A. G.; Clifford, S.; Cioslowski, J.; Stefanov, B. B.; Liu, G.; Liashenko, A.; Piskorz, P.; Komaromi, I.; Martin, R. L.; Fox, D. J.; Keith, T.; Al-Laham, M. A.; Peng, C. Y.; Nanayakkara, A.; Challacombe, M.; Gill, P. M. W.; Johnson, B.; Chen, W.; Wong, M. W.; Gonzalez, C.; Pople, J. A. Gaussian, Inc.: Pittsburgh, PA, 2003.

(10) The B3P86 Functional consists of Becke's three parameter hybrid functional (Becke, A. D. *J. Chem. Phys*. **1993**, *98*, 5648) with the nonlocal correlation provided by the Perdew 86 expression: Perdew, J. P. *Phys. Rev. B* **1986**, *33*, 8822.

(11) D95 on first row: Dunning, T. H.; Hay, P. J. In *Modern Theoretical Chemistry*; Schaefer, H. F. III, Ed.; Plenum: New York, 1976; Vol. 3, p 1. Los Alamos ECP plus DZ on Na−Bi: (a) Hay, P. J.; Wadt, W. R. *J. Chem. Phys*. **1985**, *82*, 270. (b) Wadt, W. R.; Hay, P. J. *J. Chem. Phys*. **1985**, *82*, 284. (c) Hay, P. J.; Wadt, W. R. *J. Chem. Phys*. **1985**, *82*, 299.

(12) Portmann, S.; Lüthi, H. P. *Chimia* **2000**, *54*, 766.

(13) (a) Di Bella, S.; Fragalà, I.; Ratner, M. A.; Marks, T. J. *Chem. Mater*. **1995**, *7*, 400. (b) Duan, X.-M.; Konami, H.; Okada, S.; Oikawa, H.; Matsuda, H.; Nakanishi, H. *J. Phys. Chem.* **1996**, *100*, 17780.

(14) (a) Clays, K.; Wostyn, K.; Olbrechts, G.; Persoons, A.; Watanabe, A.; Nogi, K.; Duan, X.-M.; Okada, S.; Oikawa, H.; Nakanishi, H.; Vogel, H.; Beljonne, D.; Brédas, J.-L. *J. Opt. Soc. Am. B* **2000**, *17*, 256. (b) Ray, P. C. *Chem. Phys. Lett.* **2004**, *394*, 354.

(15) Abe, J.; Shirai, Y.; Nemoto, N.; Nagase, Y. *J. Phys. Chem. B* **1997**, *101*, 1910.

(16) See for example: Cammi, R.; Tomasi, J. *J. Comput. Chem.* **1995**, *16*, 1449.

(17) Coe, B. J.; Harris, J. A.; Brunschwig, B. S.; Garín, J.; Orduna, J. Coles, S. J.; Hursthouse, M. B. *J. Am. Chem. Soc*. **2004**, *126*, 10418.

(18) Willetts, A.; Rice, J. E.; Burland, D. M.; Shelton, D. P. *J. Chem. Phys*. **1992**, *97*, 7590.

(19) (a) Oudar, J. L.; Chemla, D. S. *J. Chem. Phys*. **1977**, *16*, 1179. (b) Oudar, J. L. *J. Chem. Phys*. **1977**, *77*, 446.

(20) Tozer, D. J.; Amos, R. D.; Handy, N. C.; Roos, B. O.; Serrano-Andrés, L. *Mol. Phys*. **1999**, *97*, 859.

(21) Ray, P. C. *Chem. Phys. Lett.* **2004**, *395*, 269.

(22) The ground-state charge distributions ($|e|$) for cation **1** are as follows: from INDO/SCI 0.09 (NMe_2), 0.16 (C_6H_4), 0.06 (CH═CH), 0.69 (C_5H_4N-Me); from TD-DFT 0.03 (NMe_2), 0.44 (C_6H_4), −0.14 (CH═CH), 0.67 (C_5H_4N-Me).